

Fig. 5. A high-resolution image of  $\text{Ba}_{0.6}\text{Ti}_{2.8}\text{Al}_{1.2}\text{O}_8$  (beam direction [110]) showing regions of high (0) and low (1) correlation between the tunnels. The tunnels run in the vertical direction. Note the blurring in regions 1.

upper levels of  $x$ , derived from electron diffraction pictures.

### Discussion

We have found that stable hollandites exist only for  $x > 0.54$ . This was inferred from the fact that attempts to produce compositions with lower  $x$  resulted in the presence of  $M^{\text{IV}}\text{O}_2$  and that we never observed superperiods consistent with lower values by continuously varying  $x$  between 0.46 and 0.54.\* Direct images might be used to discriminate, but a number of

\* Note:  $x = 0.5 + y$  and  $x = 0.5 - y$  will tend to produce electron diffraction patterns with reflections at the same positions, though differing in intensities.

*Acta Cryst.* (1985). **B41**, 101-108

## Tilt and Tetrahedra Distortions in the Zeolite A Framework

BY W. DEPMEIER\*

*Chimie Appliquée, Université, Sciences II, 30 quai Ernest Ansermet, CH1211 Genève, Switzerland*

(Received 13 April 1984; accepted 30 November 1984)

### Abstract

A geometrical analysis of the zeolite A framework concerning the effects of the deviations from ideal geometry on the lattice parameter, the coordinates of the framework atoms and the  $T\text{-O-T}$  angles has been undertaken with the restriction of only one  $T$  atom present. The total deviation of the real framework from a hypothetical one, consisting of ideal  $\text{TO}_4$  tetrahedra parallel to the unit-cell edges, has been decomposed into three contributions: (i) a cooperative rotation (tilt) of the tetrahedra about axes parallel to  $\langle 100 \rangle$ ; (ii) distortions of the  $\text{O-T-O}$  angles of the

channels will be superimposed and contrasts will be blurred, unless high correlation among filling sequences along the tunnels exists. Fig. 5 is a [110] high-resolution image of the well ordered  $(\text{Ba,Ti/Ga})$  hollandite with  $x = 0.6$  showing ordered and disordered regions.

According to Bursill & Grzinic (1980),  $\text{Ba,Ti/Ga}$  hollandite with  $x = 0.4$  and  $0.5$  ( $0.8$  and  $1.0$  in their formulation based on 16 O atoms) has  $m = 2.375$  and  $m = 2.405$  (our formulation, superperiod  $mc$ ). In our model this corresponds to  $x = 0.578$  and  $0.584$ , both values being close to  $0.58$ .

This research was partly financed by the Commission of the European Communities. The authors are indebted to the workers of the Laboratory for High Voltage Electron Microscopy, Antwerp, for facilities.

### References

- BURSILL, L. A. & GRZINIC, G. (1980). *Acta Cryst.* **B36**, 2902-2913.  
 BYSTRÖM, A. & BYSTRÖM, A. M. (1950). *Acta Cryst.* **3**, 146-154.  
 CADEE, M. C. & PRODAN, A. (1979). *Mater. Res. Bull.* **14**, 613-615.  
 CHEARY, R. W., HUNT, J. V. & CALAIZIS, P. (1981). *J. Aust. Ceram. Soc.* **17**, 11-12.  
 POST, J. E., VON DREELE, R. B. & BUSECK, P. R. (1982). *Acta Cryst.* **B38**, 1056-1065.  
 SHANNON, R. D. & PREWITT, C. T. (1969). *Acta Cryst.* **B25**, 925-936.  
 SINCLAIR, W., MACLAUGHLIN, G. M. & RINGWOOD, A. E. (1980). *Acta Cryst.* **B36**, 2913-2918.

$\text{TO}_4$  tetrahedra; (iii) bond-length distortions of the tetrahedra. The  $\text{O}(1)$  atom has been used to differentiate (i) from (ii). The main results obtained are: (i) the lattice parameter passes through a maximum on varying the tilt angle;  $\angle[T\text{-O}(1)\text{-}T]$  increases,  $\angle[T\text{-O}(2)\text{-}T]$  (beyond a maximum) and  $\angle[T\text{-O}(3)\text{-}T]$  decrease with increasing tilt angle; (ii) the angular tetrahedron distortion is explained as being composed of two contributions, one of which is determined by the framework composition, the other depending essentially on the interchangeable cations. The mapping of 30 zeolite A species reveals that most of these scatter about a relaxed state with almost maximal lattice parameter and minimal deviations of the  $T\text{-O-T}$  angles from their mean value. Deviations from the relaxed state - by decreasing or increasing

\* Present address: Institut für Kristallographie, Universität, Kaiserstrasse 12, D7500 Karlsruhe, Federal Republic of Germany.

the tilt angle – result in increasing structural strains, whereby limits are set to the stability field of the zeolite A framework. A clear correlation exists between tilt angle and bond-length distortion of the  $TO_4$  tetrahedra.

### Introduction

The knowledge of the scientific and technical importance of zeolite A (for example *cf.* Breck, 1974) has resulted in a large number of publications during the last three decades concerning the structures and properties of its various hydrated or dehydrated, as-synthesized or cation-exchanged forms. However, several crystallographic aspects of their structures have been the subject of lively controversies in the past, and continue to be so (*cf.* Seff & Mellum, 1984). It is, therefore, clear that not all features of this important structure type, in particular its framework, are fully appreciated at present.

Structural changes of zeolite frameworks under the influence of temperature, pressure or variable chemical composition have recently come to attract considerable attention (*e.g.* Hazen, 1983; Smith, 1984; Fyfe, Kennedy, De Schutter & Kokotailo, 1984). In addition, correlations between the framework conformation of zeolites A and the size of exchangeable cations have been found *qualitatively* (*e.g.* Pluth & Smith, 1983*a*; Jiráček, Bosacek, Vratislav, Herden, Schöllner, Mortier, Gellens & Uytterhoeven, 1983). It seems, however, that no attempt has so far been made to describe *quantitatively* the distortions of the zeolite A framework and of their constituents, *i.e.* the  $TO_4$  tetrahedra. Therefore, it was considered a suitable moment to analyse the geometry of the framework employing a theoretical model and existing experimental data.

It was to be expected that a major contribution to the distortion of the framework would consist of cooperative rotations of the  $TO_4$  tetrahedra, so-called tilts. Furthermore, it was also found necessary to consider deviations of the tetrahedra from ideal geometry, since it has recently been revealed that these distortions can contribute substantially to the total conformation of a tetrahedra framework (Depmeier, 1984). The general strategy was, therefore, to decompose the total distortion into (i) an angular distortion of the  $TO_4$  tetrahedra, (ii) an appropriate system of cooperative rotations of the tetrahedra (tilt), (iii) bond-length distortions of the tetrahedra. An important step in the analysis was the discrimination of the tilt system from the angular tetrahedron distortion. This could be achieved by treating the  $T-O(1)$  bond as being unaffected by the changes of the  $O-T-O$  angles, whilst the other  $T-O$  bonds were regarded as being displaced relatively to  $T-O(1)$ . On the other hand, the tilt angle could be expressed in terms of  $O(1)$  only, as a simple linear

function of the angle  $T-O(1)-T$ . No attempt has been made to account for Al/Si ordering.

In the following, we will describe our model\* and some of the results of the analysis will be presented. It will then be shown that the diagram representing the lattice parameter and  $T-O-T$  angles as a function of the tilt angle lends itself to a mapping of the various zeolite A species and, finally, some aspects of this mapping will be discussed.

### The model

#### *Crystallography and structure of zeolite A: preliminary remarks*

An idealized formula of the Linde A zeolite, as a prototype of the zeolite A family, is  $Na_{12}[Al_{12}Si_{12}O_{48}].27H_2O$ . The framework consists of corner-sharing  $AlO_4$  and  $SiO_4$  tetrahedra and the part of the formula within the brackets gives its composition. The exchangeable cage cations and the zeolitic water are denoted outside the brackets. The tetrahedrally coordinated Si and Al atoms, together, will be named  $T$  atoms and no further distinction will be made between them below, since we are at present merely interested in the overall behaviour of the framework which is generally unaffected by Si/Al ordering. With this restriction, and ignoring possible minor perturbations, the zeolites A can be described pseudosymmetrically in space group  $Pm\bar{3}m$ . There is one of the above formula units in a unit cell with lattice parameter  $a = l\sqrt{(8/3)}(3 + \sqrt{2}) = 12 \text{ \AA}$  for a zeolite A with bond length  $l$ , consisting of ideal tetrahedra which are parallel to the unit-cell edges. In this case the framework atoms are in the following positions:

O(1):  $12(h)$ ;  $x_1, \frac{1}{2}, 0$  ( $x_1 = 0.2735$ )

O(2):  $12(i)$ ;  $x_2, x_2, 0$  ( $x_2 = 0.2735$ )

O(3):  $24(m)$ ;  $x_3, x_3, z_3$  ( $x_3 = 0.1133$ ;  $z_3 = 0.3867$ )

$T$ :  $24(k)$ ;  $0, y_T, z_T$  ( $y_T = 0.3867$ ;  $z_T = 0.1934$ ).

In real structures the coordinates deviate more or less from the above values depending on the tilt angle and tetrahedron distortion. A clear impression of the zeolite A structure can be obtained both from the numerous stereo plots in the literature and from Fig. 1, which shows the upper part of the so-called  $\alpha$ -cage, centred at  $\frac{1}{2}, \frac{1}{2}, \frac{1}{2}$ , which is made up of sodalite ( $\beta$ -)cages (centred at  $0, 0, 0$ ) connected by double-4-rings ( $D4R$ ; centred at  $\frac{1}{2}, 0, 0$ ). Single rings of three types occur, *viz* 4-rings, 6-rings and 8-rings ( $4R, 6R, 8R$ ). All  $TO_4$  tetrahedra are symmetrically

\* The complete geometrical analysis (Annex 1) and Table 1 containing structural information for 30 zeolite A species and references thereto have been deposited with the British Library Lending Division as Supplementary Publication No. SUP. 39900 (10pp.). Copies may be obtained through The Executive Secretary, International Union of Crystallography, 5 Abbey Square, Chester CH1 2HU, England.

equivalent and contain one O(1), one O(2) and two O(3) atoms; the latter two are related by the mirror planes parallel to {100}. O(1) belongs to two 4R and one 8R, O(2) to two 6R and one 8R and O(3) to two 4R and one 6R.

### Tetrahedron distortion

Besides bond-length distortions, the  $TO_4$  tetrahedra are subject to distortions of the O-T-O angles. These are marked in Fig. 1 and Table 2 gives the designations used in this paper. Because of symmetry, each tetrahedron has four nonequivalent angles O-T-O, three of which can be chosen independently ( $\alpha$ ,  $\beta$ ,  $\gamma$  in this study).

The tetrahedron distortion seems to have been largely neglected in former structural work on zeolites A. Now, it has recently been demonstrated (Depmeier, 1984) that the angular tetrahedron distortions may play an important role in tetrahedral frameworks, since they are capable of releasing structural strains, imposed on the framework by its own topology. In particular, it has been argued that - disregarding for a moment the influence of the cations - the most important angular distortions should occur where the strain is highest, *i.e.* in the smallest rings. In the zeolite A frameworks these are the 4R. It is, therefore, to be expected that the O-T-O angles within these rings (*i.e.*  $\alpha$  and  $\gamma$ ) are opened, whereas the remaining ones, *viz* those involving O(2) ( $\beta$ ,  $\delta$ ), are reduced in order to keep the *average*

Table 2. Designations for quantities frequently used in this work and their meanings

$l$ : mean T-O bond length	
$l_1, l_2, l_3$ : individual bond lengths T-O(1), T-O(2), T-O(3)	
$a$ : lattice parameter $\sim 12 \text{ \AA}$	
$\alpha$ : $\angle O(1)-T-O(3)$	$\rho$ : $\angle T-O(1)-T$
$\beta$ : $\angle O(1)-T-O(2)$	$\sigma$ : $\angle T-O(2)-T$
$\gamma$ : $\angle O(3)-T-O(3)$	$\tau$ : $\angle T-O(3)-T$
$\delta$ : $\angle O(2)-T-O(3)$	$\varphi$ : tilt angle

O-T-O angle at  $109.47^\circ$ . The resulting distortion of the  $TO_4$  tetrahedra is almost trigonal ( $\alpha \approx \gamma > \beta \approx \delta$ ) with O(2) forming the apex of a flattened trigonal pyramid. For reasons which become clearer below, we visualize this distortion as being brought about by moving the T-O(2) and the two T-O(3) bonds relative to T-O(1); the latter bond is regarded as being unaffected by the angular tetrahedron distortion. Repulsions occur where O atoms approach each other [O(1)-O(2), O(2)-O(3)], and an equilibrium is found which depends essentially on the topology and the composition of the framework. Table 1 (deposited) reveals that  $\alpha$  is almost constant for the 30 zeolite A species listed, giving a scatter with a formal e.s.d. of only  $1.0^\circ$  about a mean value of  $111.5^\circ$  (Table 3). No correlation of this angle with the type of exchangeable cations or with the dehydration state has been detected. This observation leads us to regard the value of  $111.5^\circ$  as characteristic for the angle  $\alpha$  of a zeolite A framework having an Al/Si ratio of 1.0.  $\alpha$  displays the trigonal distortion, whereas the other angles can be subject to perturbations by the cage cations (see below). For small deviations from the ideal tetrahedron, the trigonal distortion can conveniently be expressed by the simple relationship  $\alpha = \gamma > \beta = \delta$  with

$$\beta = 180^\circ - \arcsin\left(\frac{2}{\sqrt{3}} \sin \frac{\alpha}{2}\right). \quad (1)$$

The trigonal distortion is, thus, regarded as being determined by the framework and, in order to distinguish its contribution to the total angular distortion in what follows, we might call it the 'framework contribution to the tetrahedron distortion' or FCD.

Under certain conditions, the FCD can be superposed by a second effect which can be exemplified by describing the interactions between two basically different arrangements of the cage cations and the O atoms. Thereby it is to be noted that the 6R and 8R are favourable sites for the exchangeable cations, especially in the dehydrated state, whereas the 4R are not. We consider first a zeolite in which all 6R and 8R are occupied by cations, *e.g.* a dehydrated alkaline zeolite A. The O(2) atom at the vertex of the trigonally distorted  $TO_4$  tetrahedron is located at the intersection of two 6R and one 8R which make angles of about  $120^\circ$  with each other. It is clear that the

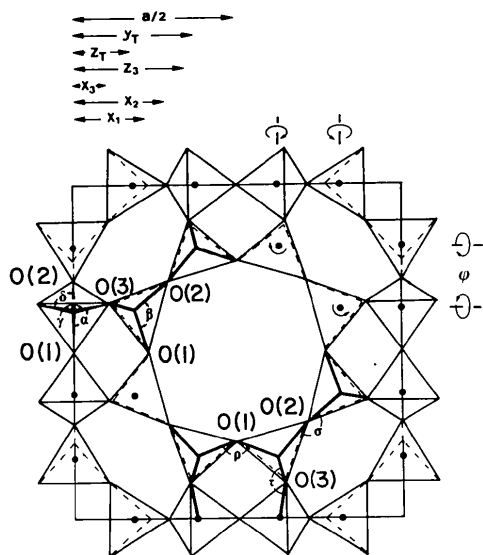


Fig. 1. The upper half of the  $\alpha$ -cage of the zeolite A framework. T atoms are marked by small solid circles, O atoms are at the corners of the tetrahedra. The angles O-T-O are marked on the upper left-hand side, the angles T-O-T on the lower right-hand side and the tilt system is indicated on the upper right-hand side of the drawing. The distances corresponding to the lattice parameter and to the coordinates of the framework atoms are shown at the top of the drawing.

Table 3. Mean values for the zeolites A listed in Table 1 and their e.s.d.'s

$l$ :	1.6636 (0.0228) Å
$\alpha$ :	111.5 (0.95)°
$\beta$ :	110.5 (4.02)
$\gamma$ :	110.3 (1.42)
$\delta$ :	106.3 (1.74)

'threefold axis' of the 'trigonal pyramid' is quite homogeneously surrounded by positive charges; therefore, (almost) no deviation from the already existing trigonal distortion will occur.

On the other hand, if the 8R are not occupied, but the 6R are - as, e.g., in the case of dehydrated Ca-exchanged zeolite A - then the cation distribution is inhomogeneous and the O(2) atom is attracted by the cations in the 6R. The resultant of the attractive forces lies in the plane of the angle  $\beta$  which is, therefore, strongly affected. Little has changed, on the other side, for  $\gamma$  and  $\delta$ . Therefore, these angles undergo only minor changes, mainly in order to adjust the mean O-T-O angle to 109.47°. The angle  $\alpha$  does not 'see' cage cations and is, furthermore, strongly controlled by the FCD. Accordingly, we assume in our model that  $\alpha$  does not change at all under the influence of the cage cations. The second effect concerns, thus, the 'cation contribution to the tetrahedron distortion' and will be abbreviated by CCD. The FCD has been regarded as being represented by  $\alpha$ ; the deviation of  $\beta$  from the value of the trigonal tetrahedron distortion - which is much more important than those of  $\gamma$  and  $\delta$  - will be considered as a measure for the CCD. The relationships described find their clear expression in the mean values and their e.s.d.'s of the angles O-T-O in Table 3. Note that in our model the effects of FCD and CCD are purely additive.

### The tilt system

The system of cooperative rotations (tilt) of the  $TO_4$  tetrahedra is indicated in the upper right-hand side of Fig. 1. In a first approximation (neglecting tetrahedron distortions), it can be described as consisting of rotations about axes which are parallel to the  $\langle 100 \rangle$  directions, pass through the T atoms and cut two opposite faces of otherwise rigid tetrahedra. The degree of cooperative rotations is measured by the tilt angle  $\varphi$ . For undistorted tetrahedra this is the angle between the tetrahedron edge O(1)-O(2) and the unit-cell edge. For distorted tetrahedra, however, this angle will be changed additionally by the 'movement' of T-O(2) relative to T-O(1) (see above). It is, therefore, a function of both, tilt and tetrahedron distortion, and certainly not a good measure of the tilt. This is precisely the reason why the T-O(1) bond has been regarded as unaffected by the tetrahedron distortion. This approach makes it possible to define the tilt angle  $\varphi$  as a simple linear function of the angle T-O(1)-T,  $\rho$ :  $\varphi = \frac{1}{2}(\rho - 109.47^\circ)$ .

It is of interest to ask why the tilt system of the zeolite A frameworks differs fundamentally from that found in the structurally closely related sodalites. In the latter the axes of rotation are perpendicular to those in zeolite A and coincide with 4 axes of the tetrahedra. In fact, cooperative rotations about these axes are also conceivable for the zeolites A. However, this would result in very unfavourable (*viz* low) values of the angle T-O(1)-T and this is probably the reason why the zeolites A prefer a tilt system which provides the possibility of opening this angle. These two structure types differ further in the fact that the T-atom coordinates are invariant in sodalites, whereas in the case of zeolites A they are not.

### Geometrical analysis

The considerations explained above allow one to investigate how tilt and tetrahedron distortions act on the lattice parameter, the coordinates of the framework atoms, the T-O-T angles and on other derived quantities. It should be noted that the usual crystallographic description of the framework (O atoms only), using the four independent fractional coordinates  $x_1, x_2, x_3, z_3$ , is equivalent to one which uses structural parameters such as the four angles  $\alpha, \beta, \gamma, \varphi$ . The latter description, however, has the advantage of being much more closely related to parameters of crystal-chemical origin; furthermore, it allows one to find simple expressions for the correlations between chemical composition (perhaps under variable temperature or pressure) and the conformation of the framework. For comparative crystal-chemical purposes the second is certainly better suited and has, therefore, been used in this work.

The distances corresponding to the lattice parameter and to the framework atom coordinates are marked in Fig. 1. The geometrical analysis consists then merely in counting the contributions of adjacent tetrahedra to these distances, taking into account, independently and consecutively, the different types of deviations from the ideal geometry, *viz* FCD, CCD, tilt and bond-length distortion. The full analysis and its results are given in Annex 1 (deposited), but the main results will be presented and discussed in the following.

### Results and discussion

For the present, we confine ourselves to only one T-O bond length  $l$ . The lattice parameter  $a$  is then given by the expression

$$a = 2l \left\{ \sin \frac{\gamma}{2} + B + 2 \sin \frac{\beta}{2} \cos \left( \arccos \left( \sin \frac{\beta}{2} \right) - 35.26^\circ + \varphi \right) \right\}, \quad (2)$$

where

$$B = \left\{ \cos^2 \frac{\gamma}{2} + 1 - 2 \cos \frac{\gamma}{2} \cos \chi \right\}^{1/2} \\ \times \cos \left\{ \arccos \left( \left( \cos \frac{\gamma}{2} - \cos \chi \right) \right. \right. \\ \left. \left. \times \left( \cos^2 \frac{\gamma}{2} + 1 - 2 \cos \frac{\gamma}{2} \cos \chi \right)^{-1/2} \right) - \psi \right\}, \quad (3)$$

with

$$\chi = 360^\circ - \beta - \arccos \left( \cos \alpha / \cos \frac{\gamma}{2} \right) \quad (4)$$

and

$$\psi = \arccos \left( \cos \alpha / \cos \frac{\gamma}{2} \right) - 125.26^\circ + \varphi. \quad (5)$$

From the definition of the tilt angle we have for  $\angle [T-O(1)-T]$

$$\rho = 109.47^\circ + 2\varphi \quad (6)$$

and the two remaining  $T-O-T$  angles are given by

$$\sigma = 180^\circ - |2\beta - 2\varphi - 199.47^\circ| \quad (7)$$

and

$$\tau = \arccos \left( \cos^2 \frac{\gamma}{2} \sin^2 \psi - \sin \gamma \cos \psi \right). \quad (8)$$

Fig. 2 shows the lattice parameter  $a$  and the  $T-O-T$  angles as functions of the tetrahedron distortion angles  $\alpha$  (full lines) and  $\beta$  (dotted lines). The tilt

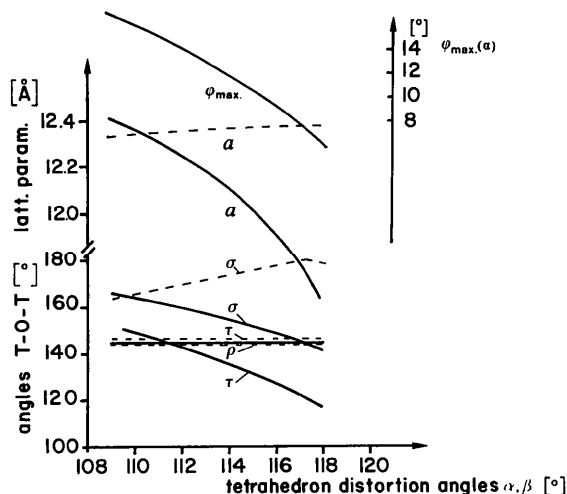


Fig. 2. The lattice parameter  $a$  and the  $T-O-T$  angles  $\rho$ ,  $\sigma$  and  $\tau$  as functions of the tetrahedron distortion angles  $\alpha$  (solid curves) and  $\beta$  (dotted curves) for a tilt angle  $\varphi = 17.5^\circ$ .  $\rho$  is independent of both  $\alpha$  and  $\beta$ ; thus, the two corresponding straight lines coincide. In addition,  $\varphi_{\max} = f(\alpha)$  is shown at the top of the diagram;  $\varphi_{\max}$  is that tilt angle at which the lattice parameter passes through a maximum.

angle  $\varphi$  has been fixed at  $17.5^\circ$ ; this value has been chosen because it corresponds approximately to a framework in the relaxed state (see below). The mean value of the bond length  $l$  ( $1.6636 \text{ \AA}$ , Table 3) has been used. For the calculations with variable  $\alpha$ , equation (1) has been employed, *i.e.* a pure trigonal distortion has been applied to the  $TO_4$  tetrahedra. In the case of variable  $\beta$ ,  $\alpha$  has been fixed at  $111.5^\circ$  (Table 3) and  $\gamma$  at  $109.5^\circ$  (*cf.* Table 1). In addition, the variation of  $\varphi_{\max}$  as a function of  $\alpha$  is shown. This quantity indicates the value of the tilt angle  $\varphi$ , at which the lattice parameter  $a$  passes through a maximum (*cf.* Fig. 3 and Annex 1). With the exception of  $\rho$  which depends only on  $\varphi$ , all quantities decrease with increasing  $\alpha$ ; thereby, the decrease is by no means negligible; *e.g.* the difference between the lattice parameters, calculated for ideal tetrahedra on the one side, and for those found in real zeolite A structures ( $\alpha = 111.5^\circ$ , Table 3) on the other, amounts to  $\sim 0.1 \text{ \AA}$  ( $\sim 0.8\%$ ). For even higher values of  $\alpha$  the calculated reduction becomes increasingly large; however, it should be noted that zeolites A with  $\alpha$  values much higher than  $111.5^\circ$  are not known so far; the corresponding curves have, therefore, only hypothetical character. This is in no way true for the dotted curves, since the large variance of  $\beta$  is an observed reality (Tables 1, 3). The angle  $\sigma$  is strongly affected by  $\beta$ , *via* the term  $2\beta$  in the linear relationship of equation (7). On the other hand,  $\rho$  and  $\tau$  are independent of  $\beta$  and the effect on  $a$  seems to be negligible.

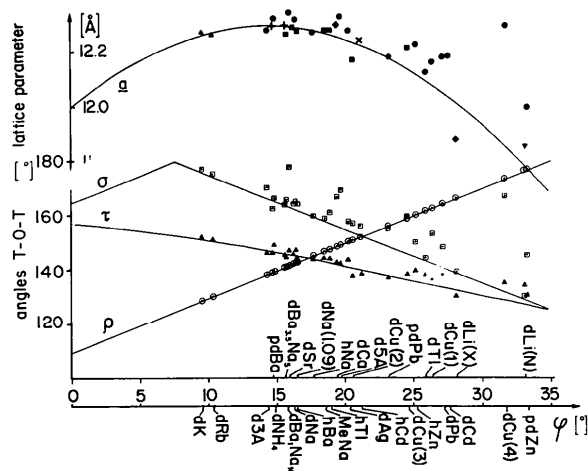


Fig. 3. The lattice parameter  $a$  and the  $T-O-T$  angles  $\rho$ ,  $\sigma$ ,  $\tau$  as functions of the tilt angle  $\varphi$ . These are shown as solid curves and have been calculated for trigonal tetrahedron distortion with  $\alpha = 111.5^\circ$  and  $l = 1.6636 \text{ \AA}$ . The diagram allows simultaneously the mapping of zeolites A; the short notations of the 30 species are found on the  $\varphi$  coordinate and correspond to those of Table 1. Solid symbols represent the observed lattice parameters; these have been normalized with  $1.6636 \text{ \AA}$ . Different symbols indicate different kinds of bond length distortion, *viz*:  $\blacktriangle$ :  $l_1 > l_3 > l_2$ ;  $\bullet$ :  $l_3 > l_2 > l_1$ ;  $\blacksquare$ :  $l_3 > l_1 > l_2$ ;  $+$ :  $l_1 = l_2 = l_3$ ;  $\times$ :  $l_3 = l_2 > l_1$ ;  $\blacklozenge$ :  $l_3 > l_2 = l_1$ ;  $\blacktriangledown$ :  $l_3 = l_1 > l_2$ .

The variation with  $\varphi$  of lattice parameter and  $T-O-T$  angles is displayed by the solid curves in Fig. 3. These have been calculated for trigonal distortions [equation (1)] using  $\alpha = 111.5^\circ$  and  $l = 1.6636 \text{ \AA}$ . The  $a = f(\varphi)$  curve is parabolically shaped with a maximum at a  $\varphi$  value which depends strongly on  $\alpha$  (cf. Fig. 2). For normally existing zeolites A, i.e.  $\text{Si}:\text{Al} \approx 1.0$ ,  $\varphi_{\text{max}}$  is of the order of  $15^\circ$ . The drop of  $a$  on both sides of the maximum is very pronounced and reaches  $\sim 0.4 \text{ \AA}$  ( $>3\%$ ) for  $\varphi = 32.5^\circ$ . Comparable percentages have been found for the sodalite framework for which the term 'partial collapse' has been coined (Pauling, 1930). It seems, therefore, reasonable to use the same expression for the zeolites A. The  $\sigma = f(\varphi)$  curve also passes through a maximum, viz where the angle  $T-O(2)-T$  becomes  $180^\circ$ . It is to be noted that, depending on the  $\varphi$  value with respect to the maximum, the angle  $\sigma$  is measured on opposite sides of the  $O(2)$  atom, in order to have  $\sigma \leq 180^\circ$ . Beyond the maximum  $\sigma$  decreases with increasing  $\varphi$ ; the inverse relationship between  $\tau$  and  $\varphi$  deviates only slightly from a straight line; the linear relationship between  $\rho$  and  $\varphi$  is due to the definition of  $\varphi$ . The mean value of the  $T-O-T$  angles (not shown in Fig. 3 for the sake of clarity) varies much less than the individual angles, keeping closely to the preferred values of  $T-O-T$  angles in aluminosilicates, i.e.  $145^\circ$ ; e.g. in the region of interest ( $10^\circ \leq \varphi \leq 35^\circ$ ) this value decreases from  $151.9$  to  $143.3^\circ$ . What seems to be of major importance for the zeolite A framework is that the sum of the deviations of the individual  $T-O-T$  angles from their mean value exhibits a deep minimum approximately between  $\varphi = 17.5$  and  $22.5^\circ$ . The minimum is, thus, shifted away from the maximum in the  $a = f(\varphi)$  curve towards higher  $\varphi$  values.

It has been noted earlier that the dependence of  $a$ ,  $\rho$  and  $\tau$  on  $\beta$  is negligible or non-existent (Fig. 2). Therefore, the corresponding curves for tetrahedron distortions other than trigonal would essentially be the same as those shown in Fig. 3. On the other hand,  $\sigma$  depends strongly on  $\beta$ . From equation (7) it follows that  $\sigma = f(\varphi)$  curves for high  $\beta$  values – as a result of strong CCD – would correspond to that shown in Fig. 3, but shifted to higher  $\varphi$  values. This means that on the right-hand side of the maximum in Fig. 3, higher  $\beta$  values result in higher  $\sigma$  values.

From the foregoing it is clear that a diagram such as Fig. 3 lends itself to a mapping of the various zeolite A species according to their framework conformation. The values for the 30 zeolites contained in Fig. 3 have been taken from the literature (see deposition footnote), but with all lattice parameters normalized with  $l = 1.6636 \text{ \AA}$  (Table 3), in order to account for small differences in the mean  $T-O$  bond lengths; the tilt angle  $\varphi$  has been calculated with equation (6). The notation used for the different species should allow an easy identification: normally the main ex-

changeable cage cation is given, preceded by  $d$  or  $h$  which stands for dehydrated or hydrated;  $p$  means partially. In case of doubt, and for additional information, the original literature should be consulted; the references are given in Table 1. The observed values match the theoretical curves very well at low tilt angles  $\varphi$ ; for higher  $\varphi$  slightly larger deviations are observed; in addition, stronger deviations occur for the  $\sigma$  values of some bivalent cations. The deviations at higher values are due to bond-length distortions (see below); the individual fugitives are explained by important CCD for these cations [cf. equation (7)]. It should be kept in mind that the perfect agreement for  $\rho$  is trivial owing to the definition of  $\varphi$ . Some features of the mapping deserve comment:

(i) There is high concentration of zeolites A in the region which is characterized by low values of the sum of the deviations,  $\sum d$ , of the  $T-O-T$  angles from their mean value. This region corresponds approximately to values of  $\varphi$  for which  $\rho$  is intermediate between  $\sigma$  and  $\tau$ .  $\sum d$  increases drastically on both sides of this region which means that some or all  $T-O-T$  angles deviate strongly from the favourable mean value of about  $145^\circ$ . The result is structural strain. Therefore, the state of minimal or low  $\sum d$  values might be called 'relaxed' (Seff, 1984), in contrast to 'strained' away from the minimum. As noted earlier, the relaxed state does not coincide exactly with the maximum in the  $a = f(\varphi)$  curve. Nevertheless, the shift is small enough so that it is reasonable to consider a diminishing lattice parameter as a clear indication of increasing structural strain and, therefore, as a sign of reduced structural stability. This inference is in good agreement with practical knowledge concerning chemical treatment of zeolites A (Seff, 1984).

On the other side, zeolite A is synthesized in the hydrated Na form which should, therefore, be distinguished by high structural stability. Indeed, Fig. 3 shows that the framework of  $h\text{Na}$  is relaxed.

(ii) A general trend is observed that small cations entail higher  $\varphi$  values and *vice versa*. The trend is valid for trigonal tetrahedron distortion ( $d\text{K}-d\text{Na}-d\text{Li}$ ), as well as for tetrahedra affected by CCD ( $d\text{Sr}-d\text{CA}$ ). However, this trend is largely superimposed by several effects of various kinds which makes it difficult to predict the final amount of partial collapse. The most important perturbing effects are: the cage cations do not necessarily occupy the centres of the single rings, for it is rather more common that they are off-centred and/or that they project into the interior of the cages; the presence of water or of adsorbed species may fundamentally change the positions of the cations. Further complications may arise from partial occupation of several cation sites and by possible preferred occupation of particular sites by certain cations (e.g. impurities). Highly covalent

bonding ( $dAg$ ) and lone-pair effects ( $dTl$ ,  $dPb$ ) seem to result in higher  $\varphi$  angles than could be supposed naively on the basis of ionic radii. Any change of the spatial distribution and of the chemical character of the cations will also change their interaction with the framework and, thereby, the conformation of the latter.

(iii) Quite generally, hydrated zeolite A species are more relaxed than the corresponding fully or partially dehydrated ones; thus, dehydration leads to enhanced structural strains. The position of the corresponding species in the diagram seems, thereby, to move away from the relaxed state without crossing it.

(iv) It is interesting to observe that the  $dK$  and  $dRb$  species have almost the same tilt angle, in spite of the considerably different atomic size. Furthermore, it has been reported (Pluth & Smith, 1983*b*) that a fully-Rb-exchanged crystalline specimen cannot be obtained; crystals rather become unstable as the Rb content increases. These observations point to the existence of a lower limit of the stability field of zeolites A at  $\varphi \approx 5\text{--}10^\circ$ . The limit might be set by the requirement that  $\rho$  should not have values much smaller than  $120\text{--}130^\circ$ . On the other hand, the approach of  $\sigma$  to  $180^\circ$  is obviously less critical, as demonstrated by several species for which  $\sigma$  is close to this value. The observation that  $T\text{--}O\text{--}T$  angles of  $\sim 180^\circ$  are more easily attainable than angles  $< 120^\circ$  is in good agreement with Fig. 6 of Gibbs, Meagher, Newton & Swanson (1981).

(v) An upper limit, at about  $\varphi = 35^\circ$ , is also observed. In this part of the diagram the agreement between observed values and theoretical curves has become unsatisfactory. The reduced agreement is accompanied by (and the result of; see below) strong bond-length distortions of the  $TO_4$  tetrahedra. This is demonstrated in Fig. 4 where the formal e.s.d. of

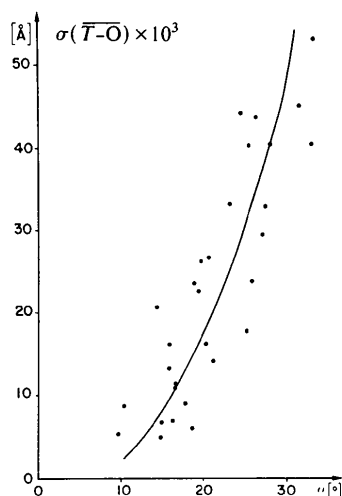


Fig. 4. The formal e.s.d. of the average  $T\text{--}O$  bond length of the 30 zeolite A species listed in Table 1 vs the tilt angle  $\varphi$ . The solid curve is a guide for the eye.

the mean  $T\text{--}O$  bond length of the zeolites A of Table 1 is plotted against the corresponding tilt angle. Both values are very well correlated and the slope of the curve suggests strongly that at  $\varphi \sim 35^\circ$  the bond-length distortion becomes infinite; hence, the zeolite A structure ceases to exist.

(vi) It has been a classical problem of zeolite A chemistry that the Ba species is the only one which is entirely stable when hydrated at 298 K, and yet unstable to dehydration at higher temperatures. The explanation given (Kim, Subramanian, Firor & Seff, 1980) is that, as the  $Ba^{2+}$  ions, unlike  $Ca^{2+}$  or  $Sr^{2+}$ , are less suited to  $6R$  sites, they rather prefer to occupy  $8R$ . This view is nicely supported by Fig. 3: the  $hBa$  species is in a quite well relaxed conformation; clearly, the coordination requirements of the  $Ba^{2+}$  ions are, to a large extent, met by the water. On partial dehydration ( $pdBa$ ) the framework becomes strained, which is quite normal in view of (iii). More important is that  $\sigma$  of  $pdBa$  is smaller than that of the trigonal tetrahedron distortion. In fact,  $pdBa$  is the only species in the whole diagram for which this is true. This anomaly is easily explained, following the opposite arguments used in the discussion of the CCD, by the presence of Ba in the  $8R$ , accompanied by depopulation of the  $6R$ . In  $pdBa$  all available  $8R$  are already occupied by Ba; further dehydration must lead to more and more  $Ba^{2+}$  ions in unfavourable sites and, thereby, to growing instability. Thus, it is plausible that fully dehydrated Ba zeolite A cannot exist.

(vii) Tentatively, different symbols have been used for the points representing the lattice parameters in Fig. 3. These symbols indicate different patterns of bond-length distortion. Some trends for the distribution of these patterns appear in outlines; however, it would be premature to make definite statements about this point at the moment.

The geometrical analysis in Annex 1 has been made distinguishing individual bond lengths. The effects of replacing individual bond lengths by the mean bond length  $l$  have been investigated. Not surprisingly, the discrepancies between the two models increase quite strongly with increasing bond-length distortion (compare right-hand side of Fig. 3 with Fig. 4). For small bond-length distortion, however, the disagreement is almost negligible; e.g. for  $dSr$  the difference in the lattice parameters is 0.12%, whereas for the coordinates  $x_1$ ,  $x_2$ ,  $x_3$ ,  $z_3$  it is 0.53, 0.50, 0.90 and 0.17%, respectively. Of course, no difference between the two models occurs for the  $T\text{--}O\text{--}T$  angles.

An important value for estimating molecular sieve properties of zeolite A is the size of the aperture of the  $8R$ . This is limited by the shorter of the distances between opposite O(1) or O(2) atoms, respectively, across the  $8R$ . The corresponding formulae are given in Annex 1. It should be noted that the aperture depends strongly on  $\varphi$ . The corresponding curve is

characterized by a pronounced maximum and falls off quite strongly on both sides; e.g. for  $dK$  (Pluth & Smith, 1979) the maximum is at  $\varphi = 21^\circ$  and the descent of the curve is of the order of  $1\%/1^\circ\Delta\varphi$ ; i.e. the aperture of the  $8R$  of this zeolite ( $\varphi = 9.6^\circ$ ) is reduced by  $\sim 10\%$ , compared with the maximal value, merely because of the effects of the tilt.

A program which models the zeolite A framework is available (Berset & Depmeier, 1984).

It is a pleasure to thank M. G. Berset for programming the content of Annex 1, M. R. Cros for the drawings, M. E. Burkhardt for the photographs, Professor K. Seff and the anonymous referees for helpful remarks and Dr H. D. Flack for reading the manuscript. This work has been supported by the Swiss National Science Foundation under contract No. 2.833-0.83.

#### References

- BERSET, G. & DEPMEIER, W. (1984). *ZEOLIT*. A Fortran program for modelling the zeolite A framework. Available on request.
- BRECK, D. W. (1974). *Zeolite Molecular Sieves*. New York: John Wiley.
- DEPMEIER, W. (1984). *Acta Cryst.* **B40**, 185-191.
- FYFE, C. A., KENNEDY, G. J., DE SCHUTTER, C. T. & KOKOTAILO, G. T. (1984). *J. Chem. Soc. Chem. Commun.* pp. 541-542.
- GIBBS, G. V., MEAGHER, E. P., NEWTON, M. D. & SWANSON, D. K. (1981). *Structure and Bonding in Crystals*, Vol. I, edited by M. O'KEEFFE & A. NAVROTSKY, pp. 195-225. New York: Academic Press.
- HAZEN, R. M. (1983). *Science*, **219**, 1065-1067.
- JIRÁK, Z., BOSACEK, V., VRATISLAV, S., HERDEN, H., SCHÖLLNER, R., MORTIER, W. J., GELLENS, L. & UYTTERHOEVEN, J. B. (1983). *Zeolites*, **3**, 255-258.
- KIM, Y., SUBRAMANIAN, V., FIROR, R. L. & SEFF, K. (1980). *Am. Chem. Soc. Symp. Ser.* No. 135, pp. 137-153.
- PAULING, L. (1930). *Z. Kristallogr.* **74**, 213-225.
- PLUTH, J. J. & SMITH, J. V. (1979). *J. Phys. Chem.* **83**, 741-749.
- PLUTH, J. J. & SMITH, J. V. (1983a). *J. Am. Chem. Soc.* **105**, 1192-1195.
- PLUTH, J. J. & SMITH, J. V. (1983b). *J. Am. Chem. Soc.* **105**, 2621-2624.
- SEFF, K. (1984). Private communication.
- SEFF, K. & MELLUM, M. D. (1984). *J. Phys. Chem.* **88**, 3560-3563.
- SMITH, J. V. (1984). Private communication.

*Acta Cryst.* (1985). **B41**, 108-112

## Electron Microscopy of Defects and Disorder in $BaGa_{12}O_{19}$

BY T. WAGNER AND M. O'KEEFFE

*Department of Chemistry, Arizona State University, Tempe, Arizona 85287, USA*

(Received 31 July 1984; accepted 30 November 1984)

#### Abstract

$BaGa_{12}O_{19}$  has been examined by high-resolution electron microscopy. It has a disordered structure based on a supercell of the magnetoplumbite structure. Disorder consists of the occurrence of different choices of origin of the supercell both within and between (0001) layers. Antiphase boundaries and more complex structures caused by interaction of the various types of defect are also found. It is suggested that the superstructure arises from a modification of the spinel blocks. Chemical microanalysis yields the atomic ratio  $Ga/Ba = 11.7 \pm 0.8$ .

#### Introduction

Adelsköld (1938) first determined the structure of magnetoplumbite,  $BaFe_{12}O_{19}$ , and a large number of compounds have since been reported to be isostructural (Morgan & Cirlin, 1982). Adelsköld found the symmetry to be  $P6_3/mmc$ , but subsequent investigators have found evidence for lower symmetry in some cases. Thus Verstegen (1973) observed some

reflections  $000l$  with  $l$  odd in the powder pattern of  $BaGa_{12}O_{19}$ , a compound which is the subject of the present study. It is now well established that ' $BaAl_{11}O_{19}$ ' is in fact two distinct phases (I and II) with compositions different from the ideal one. These have recently been the subject of several electron microscope investigations (Morgan & Shaw, 1983; Iyi, Takekawa, Bando & Kimura, 1983; Yamamoto & O'Keeffe, 1984). Yamamoto & O'Keeffe showed from convergent-beam electron diffraction that phase I indeed had symmetry  $P6_3/mmc$  but that phase II had trigonal or lower symmetry. All the electron microscope studies of phase II also found imperfect ordering corresponding to formation of supercell  $\sqrt{3}a \times \sqrt{3}a \times c$ . Recently Ganapathi, Gopalakrishnan & Rao (1984) reported the evidence of the existence of phase II crystals of  $BaFe_{12}O_{19}$ , and Bovin (1981) has also observed phase II behavior in plumboferrite, ' $PbFe_4O_7$ '. To date there is no satisfactory explanation for the occurrence of a superstructure or indeed even for the composition of the crystals.

In the magnetoplumbite structure there are layers with composition  $ABO_3$  (here  $A$  is a large atom such